

Flexural Performance of CFRP-Bamboo Scrimber Composite Beams

Xizhi Wu^{1,2}, Xueyou Huang³, Xianjun Li^{1,*} and Yiqiang Wu¹

¹College of Materials Science and Engineering, Central South University of Forestry and Technology, Changsha, 410082, China.

²Yihua Life Science and Technology Co., Ltd., Shantou, 515000, China.

³Hunan Special Equipment Inspection and Testing Institute, Changsha, 410082, China.

*Corresponding Author: Xianjun Li. Email: lxjmu@163.com.

Abstract: This study presents a new structure made up of bamboo scrimber and carbon fiber reinforced polymer (CFRP) to address the low stiffness and strength of bamboo scrimbers. Three-point bending test and finite element model were conducted to study the failure mode, strain-displacement relationship, load-displacement relationship and relationships between strain distribution, contact pressure and deflection, and adhesive debonding. The results indicated that the flexural modulus and static flexural strength of the composite beams were effectively increased thanks to the CFRP sheets. The flexural modulus of the composite specimens were 2.33-2.94 times that of bamboo scrimber beams, and the flexural strength were 1.49-1.58 times that of bamboo scrimber beams. Adhesive debonding had a great influence on the strain distribution and deflection of the composite specimens. It was an important factor for the failure of the CFRP-bamboo scrimber composite specimens. According to the finite element simulation, the strain distribution, contact pressure and deflection also greatly changed with the adhesive debonding. After complete peeling, the deflection of the specimen was 3.09 times that of the unpeeled because it was no longer an integral beam.

Keywords: Bamboo scrimber; carbon fiber reinforced polymer (CFRP); flexural performance; adhesive debonding

1 Introduction

With increasing demands on green buildings, bamboo is becoming an interesting and promising construction material [1,2]. The bamboo is a natural biomass composite material that can be regenerated after being cut and can be degraded after being discarded. Bamboo not only has a fast growing rate, being ready for harvest in 3-5 years, but also has a high strength-to-weight ratio, compared with other traditional buildings such as steel and concrete [3,4]. However, the use of natural bamboo as construction material is limited mainly because of small diameter, hollow wall and easy to crack. To overcome these constraints, bamboo scrimber and laminated bamboo are typical composite products based bamboo fiber. The bamboo scrimber is made up of bamboo bundles or fiberized bamboo veneers as a unit, glued and pressed into plate or square material [5-8].

The bamboo scrimber has been extensively applied in indoor decoration, garden landscape, outdoor anti-corrosion flooring, etc., but its rigidity and strength are smaller than traditional steel, which is difficult to meet the requirements of long-span structures [9,10]. Therefore, potential strengthening technology to enhance the stiffness and strength of bamboo scrimber needs to be explored. There were various strengthening techniques in previous studies for wood and bamboo structure. For instance, Luca et al. [11] investigated the flexural behavior of reinforced and reinforced-prestressed glue laminated timber beams with steel bars. The experimental results demonstrated that flexural strength can be improved by

strengthening beams with simple or prestressed steel bars. A remarkable observation in the study was a pronounced ductile zone in a reinforced beam and a completely brittle zone in an unreinforced beam. Yong et al. [12] studied the flexural performance of the reinforced bamboo scrimber composite (RBSC) beam combining the bamboo element and the steel bars. The results indicated that the reinforcement and the bamboo elements could firmly form an integrated composite cross-section. The failure modes, ultimate load and cross-section stiffness of the RBSC beams were significantly correlated to the diameter of reinforcement and the heat treatment of bamboo bundle. Fiber reinforced polymer (FRP) composites are an alternative to metal used to reinforce wood and bamboo structures. Nadir et al. [13] discussed the flexural properties of laminated wood beams that are strengthened with carbon fiber-reinforced polymer (CFRP) and glass fiber-reinforced polymer (GFRP) composite sheets. The results indicated a significant increase in the flexural strength and stiffness of FRP-wood composite beams. Wei et al. presented a bamboo structure that was reinforced with bars [14-16]. The application of bars in the tensile regions of bamboo beams significantly increased the load-carrying capacity and section stiffness and improved the utilization of the compression plastic behavior of bamboo. Zhou et al. [17-20] carried out the four-point bending test of CFRP reinforced bamboo scrimber beam. The results indicated that the deformation of the specimens were nonlinear when the stress of the outermost fibers exceeded the limit of compression resistance in the compression zone and the fibers at the bottom of the component were broken when the outermost fibers exceeded the limit of tensile strength in the tension zone. Yang et al. [21] studied bamboo scrimber beams that were strengthened by fiber-reinforced polymer (FRP) composite sheets embedded in the internal tensile region with an additional bamboo plate. Four-point bending tests were conducted to determine the failure modes, the load-displacement relationship, the load carrying capacity and the flexural rigidity of reinforced bamboo scrimber beams. The results indicated that the failure of the strengthened beams started with tensile fractures on the bottom bamboo plates, and no slipping was observed between the strengthening materials and the original bamboo beams prior to the rupturing of the bamboo plates. Li et al. [22,23] studied the efficiency of AFRP reinforcement on parallel bamboo strand lumber beams. The results showed that AFRP can effectively improve the flexural mechanical properties of parallel bamboo strand lumber beams. When the cloth ratio was 0.48, the deflection of the specimens reached its maximum.

The above literatures used FRP bars or thin FRP sheets to reinforce bamboo and wood beams. However, there are few studied on the bending of thick CFRP sheets to reinforce bamboo scrimber beams, which can give a boost to the flexural performance of the bamboo scrimber beam. This study presents a new type of bamboo scrimber beams combining bamboo scrimber sheets with thick CFRP sheets. Three-point bending tests were conducted to determine the failure mode, strain-displacement relationship, load-displacement relationship, static flexural modulus and static flexural strength. Then, the influence of adhesive strip on the deformation of composite beams was also discussed through finite element model.

2 Experimental Tests

2.1 Materials

In this paper, the bamboo scrimber was manufactured by Yiyang Taohuajiang Bamboo Industry Co., Ltd. The Moso bamboo (*Phyllostachys pubescens*), aged 3-4 years, was harvested from Yiyang county, Hunan province, in the south part of China. The bamboo was passed through a rolling machine along the grain direction to obtain the oriented bamboo bundles. The bamboo bundles were heated using steam at 130°C for 140 min. The impregnated adhesive was the water-soluble phenolic resin adhesive of Guangdong Taier Co., Ltd. The mechanical properties are shown in Tab. 1.

The CFRP material used in the tests was CUDP- H150/T700-E7, which had a Young's modulus of 110 GPa, and a thickness of 0.15 mm for each ply. The mechanical properties are shown in Tab. 1.

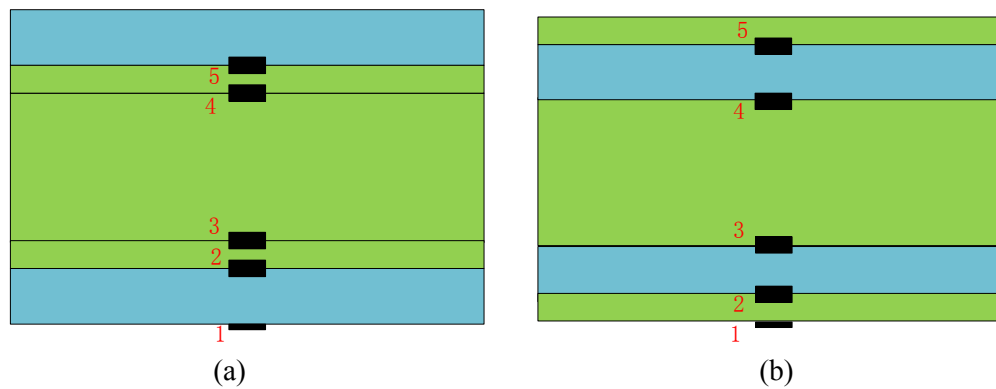
The epoxy resin used in bonding CFRP sheets and bamboo scrimber sheets was Sikadur-330. The thickness of the epoxy resin was 0.1 mm.

Table 1: The performance of CFRP and bamboo scrimber

Name	Longitudinal elastic modulus (MPa)	Transverse elastic modulus (MPa)	Longitudinal shear modulus (MPa)	Transverse shear modulus (MPa)	Poisson's ratio
CFRP	110000	7600	4500	3400	0.30
bamboo scrimber	22000	3000	1500	1500	0.32

2.2 Specimen Preparation

Three types of beams with a dimension of 600 mm × 30 mm × 30 mm were used for bending tests, which were shown in Tab. 2 and Fig. 1. Group 0 were the comparative beams, Group 1 and Group 2 were CFRP-bamboo scrimber composite beams, and each group included three specimens. In Fig. 1, the blue represented CFRP and the green represented bamboo scrimber. The total thickness of CFRP of Group 1 was the same as Group 2, but their layering modes were different. The layering mode of Group 1 was B-C-B-C-B, and the layering mode of Group 2 was C-B-B-B-C, where B represented bamboo scrimber, C represented CFRP, the thickness of each layer of CFRP was 4 mm, and the thickness of the outermost layers of bamboo scrimber were 2 mm.

**Figure 1:** Combination design of specimens and strain gauge positions: (a) Group 1, (b) Group 2**Table 2:** The specimen details of the bending test

Number	Type	Layering mode	Thickness of CFRP (mm)	Sizes (mm)	Number
0	bamboo scrimber beam	none	0	600 × 30 × 30	3
1	Composite Beams	B-C-B-C-B	8	600 × 30 × 30	3
2	Composite Beams	C-B-B-B-C	8	600 × 30 × 30	3

The bamboo scrimber beams (Specimen 0-1 ~ 0-3) were hot pressed for one time, and other beams were reheated and cured with the bamboo scrimber sheets and CFRP sheets. The process of making CFRP-bamboo scrimber composite (CBSC) beams was as follows: (1) Preparation of the bamboo scrimber sheets: pass natural bamboo tubes through a rolling machine along the grain direction, flatten along the longitudinal fiber direction to obtain the oriented bamboo bundle, use steam to heat them at 130°C for 140 min, immerse them in resin for about 10-15 min at room temperature, dry for 8 h at room temperature, make them into plates using a hot pressing machine, and then saw them into required sizes [9,10,15]. (2) Preparation of CFRP sheets: cut the prepreg CFRP into required sizes, bond them into sheets for the required thickness, and cure them in an incubator for 90 min at 120°C. (3) Preparation of CBSC beams: polish the bamboo scrimber sheets and CFRP sheets with 240 Grit sandpaper to remove oil stains, etc., from the surface to form a certain surface roughness to enhance the bonding force, scrub the surface of the

bamboo scrimber and CFRP sheets with alcohol to further remove grease and contaminants, mix Component A and B of Sikadur-330 in a certain proportion and stir it for about 5 min, apply the adhesive to the surface of the bamboo scrimber sheets with a special brush to adhere the element, make sure the thickness of the adhesive layer is 0.3 mm, and then cure it in the incubator for 90 min at 45°C [12].

2.3 Bending Test

A three-point bending test was adopted in accordance with Chinese national standard GB/T 50329-2012 [24]. The schematic drawing and photo of the bending test are shown in Figs. 2(a) and (b), respectively. The distance between two supports was 440 mm, the two supporting rollers and the loading roller were semi-cylindrical with radius 30 mm, and the loading roller was located in the center of the specimen. A universal test machine with a load capacity 100 kN supplied by MTS System Corporation (Minnesota, USA) was used to investigate the mechanical performances of CBSC beams under bending.

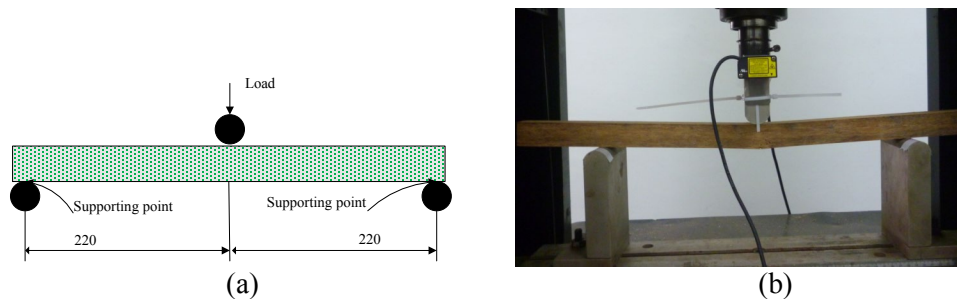


Figure 2: Three-point bending test: (a) schematic drawing; (b) photo

Test steps were as follows: (1) Symmetrically placed the specimen in a mid-span position. (2) Before the formal loading, applied an initial load of 5% of the maximum load to the specimen to ensure that it is in normal working condition. (3) During the formal loading, the speed was controlled by displacement changes within 2 mm/min until the specimen was damaged.

In the test, the static flexural strength can be calculated with formula 1 (MPa):

$$\sigma_{\max} = \frac{3P_{\max}L}{2bh^2} \quad (1)$$

where, P_{\max} is the ultimate load (N);

L is the distance between the left and right supporting points (mm);

b is the width of the specimen (mm);

h is the height of the specimen (mm).

The static flexural modulus can be calculated with formula 2 (MPa):

$$E = \frac{L^3 \Delta F}{48I \Delta w} \quad (2)$$

$$I = \frac{bh^3}{12} \quad (3)$$

where, ΔF is the varying load (N);

Δw is the varying deflection at mid-span position (mm);

I is the cross-sectional moment of inertia (mm⁴).

To monitor the starting position of specimen damage, strain gauges were attached as shown in Fig. 1. For all specimens, a strain gauge along longitudinal direction was attached to the bottom at the mid-span position recorded as Point 1. Strain gauges along longitudinal direction were attached at the mid-span of the adhesives between the adjacent layers, recorded as Point 2, 3, 4, and 5, respectively. The strain gauge was BE120-3AA of AVIC Electric Instrument Co., Ltd. with a sensitive grid length of 3 mm and a

nominal resistance of 120 Ω . The 9235 dynamic module of an US-based company National Instruments (NI) was also used to receive strain data.

3 Experimental Results

3.1 Failure Modes

The failure mode of all specimens is shown in Tab. 3. The failure mode of the bamboo scrimber beam 0-1 is shown in Fig. 3 where the bamboo fibers begin to break at the lower surface of the beam at the mid-span position, and gradually expand vertically to the middle and upper parts of the beam. At the same time, several horizontal cracks lead to delamination failure. No visible local curvature or breakage was detected in the compression zone. A similar failure mechanism appeared in the studies of timber glulam beams by Glišović et al. [25].

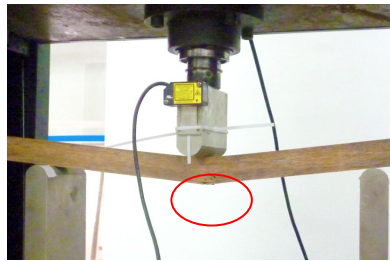


Figure 3: Failure mode of the bamboo scrimber beam

The final failure mode of CBSC beam 2-1 is shown in Fig. 4. During the test, a large area of bonding interface debonded at the first adhesive layer between the CFRP and the bamboo scrimber layer (the bonding interface is sequentially referred to as the first, second and so on from top to bottom) followed by a large blasting sound, and the universal test machine was automatically reset, with no visible damage detected on the CFRP plates or the bamboo scrimber plates. Other CBSC beams had the same failure mode but with different failure positions. For example, the failure position of Specimen 1-1 was at the third adhesive layer. However, Yang et al. [21] presented a different failure process where slipping did not occur between the strengthening materials and the original bamboo beams prior to the rupturing of the bamboo plates where only 1~3 layers FRP were applied. The reason for the difference may be that as the thickness of CFRP increases, the interface becomes more prone to peeling off.

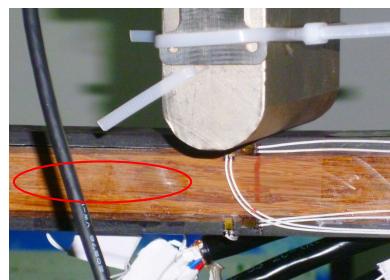


Figure 4: Final failure mode of CBSC beams 2-1

The failure mode of interface debonding is shown in Fig. 5. The surface debonding of Specimen 2-1 occurs at the first adhesive layer, where a large area of adhesive remains on the surface of the bamboo scrimber and CFRP, and the bamboo scrimber with a thickness of 2 mm is torn into two halves, indicating that the bonding force of interface between the adhesive and CFRP or the bamboo scrimber is less than the mechanical properties of the adhesive layer, and when the bamboo scrimber is very thin, the bonding force of the inner adhesive of the bamboo scrimber is less than the interfacial adhesive between the laminas. Compared with Specimen 2-1, the surface debonding of Specimen 1-1 occurs at the third

adhesive layer, where the single continuous area of the adhesive peeling is small, and more pieces of CFRP and bamboo scrimber remain on the debonding surfaces.

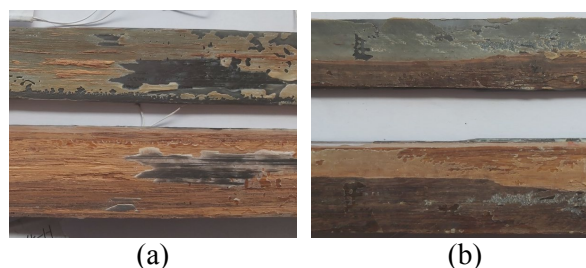


Figure 5: Failure mode of interface debonding: (a) 1-1, (b) 2-1

3.2 Load-Displacement Curves

Fig. 6 shows the load-displacement curves of the bamboo scrimber and CBSC specimens where (1) the deformation process of the bamboo scrimber beam can be divided into three stages. The first is the linear elastic stage where the curve is almost linear from the beginning to about 50% of the loading process. The second stage features stiffness degradation where the flexural stiffness slowly decreases as load climbs from the end of the first stage to the limit load with no obvious damage observed on the outer surface of the bamboo scrimber beam. There are occasionally weak noises that may be caused by the damage of fibers or weak bonding interface of fibers inside the bamboo scrimber. The deflection of the ultimate load is 14.5 mm. The third is the failure stage. As the load reaches its limit, the specimen produces a loud noise with the load-displacement curve dropping a bit due to the brittle fracture in the bottom tension area, but the bamboo scrimber beam can continue bearing load. With the increase of the deflection, the specimen intermittently produces large noises each accompanying a slight drop in the load-displacement curve. The maximum deflection is 42.8 mm, 2.95 times that at the ultimate load, showing that the bamboo scrimber beam is damaged gradually. (2) The deformation process of CBSC beam can boil down to two stages. The first is the linear elastic stage where the load-displacement curve is almost linear. The second features adhesive debonding. With the load increasing, the specimen produces small noises, and the load-displacement curve suddenly drops by a small margin, which may be due to local adhesive debonding. Then the curve becomes nonlinear as the load increases. The specimen produces a loud noise as the curve sharply drops due to a large area of the adhesive debonding, and the universal testing machine is automatically reset. The specimen can still bear load in the end. (3) With the same section, the linear elastic slope of CBSC beams are much larger than that of bamboo scrimber beam, which means that CFRP can help boost the linear elastic stiffness of bamboo scrimber beam. (4) At the linear elastic stage, the maximum deflection of CBSC beam 1-1 is 6.9 mm, CBSC beam 2-1 6.3 mm, and the bamboo scrimber beam 0-1 7.3 mm, so when CBSC beam 1-1 and 2-1 are destroyed, the bamboo scrimber is basically at the linear elastic stage with no stiffness degradation.

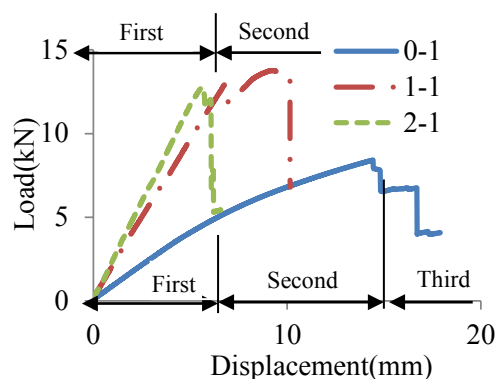


Figure 6: Load-displacement curves of the bamboo scrimber and CBSC specimens

3.3 Strain-Displacement Curves

The load-displacement and strain-displacement curves of the bamboo scrimber Specimen 0-1 are shown in Fig. 7. For the strain curve, the initial stage is almost linear until the elastic limit. At around 14.5 mm, the strain value plummets to a negative that is beyond the measuring range (± 0.02), indicating that the strain gauge has been destroyed. For the load-displacement curve, it is smooth without abrupt changes until the sudden drop of the strain when the load history curve begins to deform accordingly. Hence, it can be found that the failure of bamboo scrimber beams is caused by the breakage of bamboo fiber on the bottom surface of the beams at the mid-span position. This conclusion is also consistent with the observed failure process.

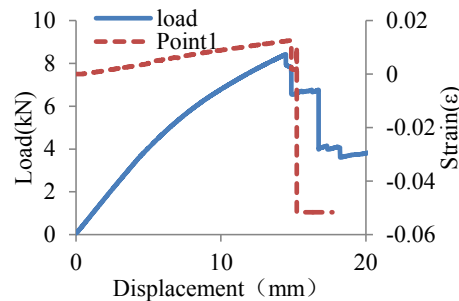


Figure 7: Load-displacement and strain-displacement curves of the bamboo scrimber specimen 0-1

Fig. 8 shows the load-displacement and strain-displacement curves of CBSC Specimen 1-1. For the strain curves, the initial stage for all test points are almost linear until an abrupt change in the load-displacement curve. The strain slope at Point 4 is greater than that at Point 3, meaning that for the two centrosymmetric adhesive interfaces, the load on the one with compressive stress is greater than that on the other with tensile stress. At around 6.9 mm, there is a transient descent process in the load-displacement curve and strain-displacement curve of all test points, and the change in the strain at Point 4 is greater than that at Point 3, indicating the softening or damage occurs locally on the adhesive interfaces which is severer for the interface with compressive stress than the one with tensile stress. As the loading continues, at about 10.62 mm, the strain value at Point 3 suddenly decreases from a positive value to a negative value which is beyond the measuring range, and the strain at Point 4 has a small decline, meaning that the strain gauge at Point 3 has been destroyed, and large-scale peeling occurs to the interface between the second layer of CFRP and the second bamboo scrimber sheet. Contrasted with Specimen 0-1, the strain at Point 1 for Specimen 1-1 is always in the normal measurement range with no sudden changes, indicating that the CFRP at bottom is not broken.

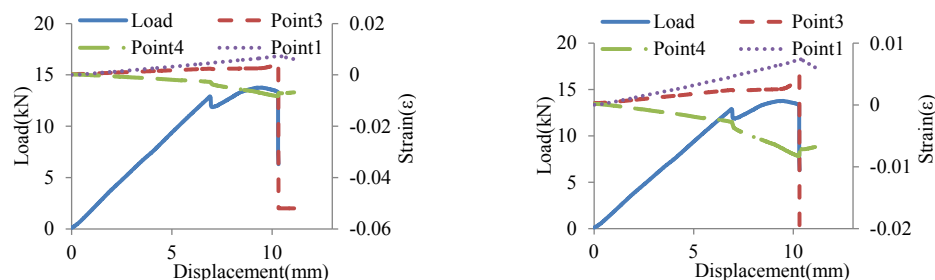


Figure 8: Load-displacement and strain-displacement curves of CBSC specimen 1-1

3.4 Flexural Performance Analysis

The mechanical properties of all specimens that are obtained from the three-point bending test are shown in Tab. 3. The average static flexural modulus of the bamboo scrimber beams is 12240 MPa, and the average static modulus of the first group of CBSC specimens is 28580 MPa, 2.33 times the former.

The main reason is that the elastic modulus of CFRP is much larger than that of the recombinant bamboo. The average static modulus of the second group of CBSC specimens is 35947 MPa, which is 2.94 times that of the reconstituted bamboo and 1.26 times that of the first group of CBSC specimens, because the CFRP sheets of the second group are at the outermost to make it more difficult to deform.

The average static flexural strength of the bamboo scrimber beams is 175.17 MPa, and that of the first group of CBSC specimens is 276.39 MPa, 1.58 times the former. The average static modulus of the second group of CBSC specimens is 261.38 MPa, which is 1.49 times that of the first group of CBSC specimens. The enhancement of static flexural strength of CBSC specimens is smaller than that of static flexural modulus as a result of the premature peeling of the bonding interface of the composite specimen, which reduces the static bending strength of the composite specimen.

Table 3: Mechanical properties of three-point bending test of all specimens

Number	Thickness of CFRP (mm)	Ultimate load (N)	Deflection (mm)	Static flexural strength (MPa)	Static flexural modulus (MPa)	Failure modes
0-1	0	10224	14.50	204.48	13032	bamboo fibers break
0-2	0	8418	14.73	168.36	11779	bamboo fibers break
0-3	0	7634	14.06	152.68	11909	bamboo fibers break
1-1	8	13768	10.62	282.71	28593	interface debonding
1-2	8	12538	10.37	257.45	28365	interface debonding
1-3	8	14075	10.85	289.01	28782	interface debonding
2-1	8	12714	6.86	257.72	35450	interface debonding
2-2	8	12806	10.37	259.58	36361	interface debonding
2-3	8	13164	10.85	266.84	36032	interface debonding

4 Effect of Interface Peeling of CBSC Beams

4.1 Finite Element Model

It can be seen from the failure mode, load-displacement curve and strain-displacement curve of the test that interface peeling is an important cause for the failure of the composite structure. To study the influence of interface peeling on the CBSC beams, it is necessary to establish a finite element model of the CBSC beam factoring in interface peeling while avoiding looking at how the interface is peeled off.

A CBSC beam is a multi-layer composite consisting of bamboo scrimber, adhesive layer and CFRP. This paper sets up a finite element model with Specimen 1-1 shown in Fig. 9. To simplify the simulation, it only modeled the interface peeling between the second sheet of bamboo scrimber and the second CFRP sheet. Adhesive layers were neglected as they were too thin to have much influence on the bearing capacity of the CBSC beam. Both the bamboo scrimber and CFRP were fiber reinforced composites modeled using eight-node reduced integral hexahedral element (C3D8R). According to the test results, the bamboo scrimber and CFRP are in a linear deformation when the interface is peeled off, so the finite element model only needs to consider its linear elastic properties, which are shown in Section 2.1. In order to analyze the influence of the peeling of the interface, when the adhesive layer was not peeled off, the upper and lower nodes of the interface were tied together with the same displacements. When the adhesive layer was peeled off, the upper and lower elements of the stripping area were simulated through surface-to-surface contact, where only positive pressure and tangential friction could be transmitted between them. The size of the elements was 1-3 mm, and the model had a total of 24180 elements and 37026 nodes. The translational DOFs of X, Y and Z were constrained for the left nodes of support, the translational DOFs of Y and Z were constrained for the right nodes of support, and a concentrated load of 13.768 kN was applied in the center of the composite beam.

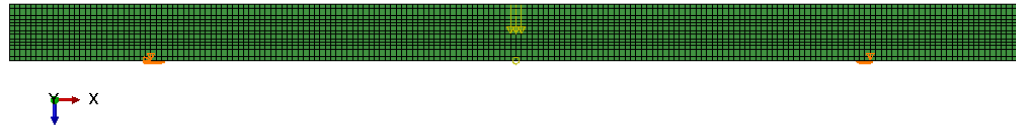


Figure 9: Finite element model of specimen 1-1

4.2 Simulation Result Analysis

Fig. 10 shows the X-direction LE (logarithmic strain) of Specimen 1-1 when the adhesive between the second sheet of bamboo scrimber and the second CFRP sheet is intact and completely debonded. The maximum strain is 7.35×10^{-3} at the bottom and mid-span of specimen, and the minimum is -1.04×10^{-2} at the top and mid-span of specimen, which conforms to the stress distribution of the three-point bending of the beam. After the adhesive is completely debonded, the maximum strain is 2.47×10^{-2} at the bottom and mid-span of the second sheet of the bamboo scrimber, much bigger than the strain at the mid-span of the second CFRP sheet. The minimum strain of the specimen is -1.72×10^{-2} at the top and mid-span of the specimen. After the adhesive completely stripping, the strain on Specimen 1-1 is not in line with the stress distribution of the three-point bending of the beam, but similar to that of the two independent beams. The maximum strain on the debonded specimen is 3.36 times that on the intact specimen, and the minimum is 1.65 times that on the intact specimen. The maximum strain shows more significant increase after stripping.

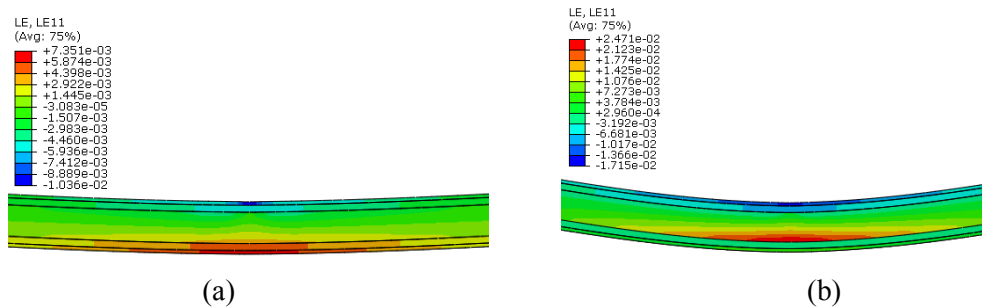


Figure 10: X-direction LE of Specimen 1-1: (a) intact, (b) completely debonded

Fig. 11 shows the X-direction strains of the second CFRP sheet with a distance of 150 mm from mid-span where the maximum strain and the minimum strain of a, b, c, and d are the same, respectively, maximum in red and minimum in blue. The adhesive between the second sheet of bamboo scrimber and the second CFRP sheet symmetrically debonds about the mid-span position. The X-direction strain gradient of the second CFRP sheet changes significantly as tensile strain when the adhesive layer is not peeled off, and the strain at the bottom of the mid-span is 5.12×10^{-3} . When the adhesive layer is symmetrically debonded by a total length of 100 mm, the X-direction strain gradient of the second CFRP sheet does not change too much as tensile strain, and the strain at the bottom of the mid-span is 4.75×10^{-3} . When the adhesive layer is symmetrically debonded by a total length of 500 mm, the X-direction strain gradient of the second CFRP sheet has even smaller changes as tensile stress, and the strain at the bottom of the mid-span is 1.88×10^{-3} . When the adhesive layer is completely debonded, the X-direction strain of CFRP becomes compressive stress, and the strain at the bottom of the mid-position becomes -2.95×10^{-4} , significantly different from the strain before peeling. The relationships between LE of the second CFRP at mid-span position and the length of the adhesive layer debonding are shown in Fig. 12. The LE at the mid-span position decreases at a hiking speed as the length of the stripped adhesive layer increases.

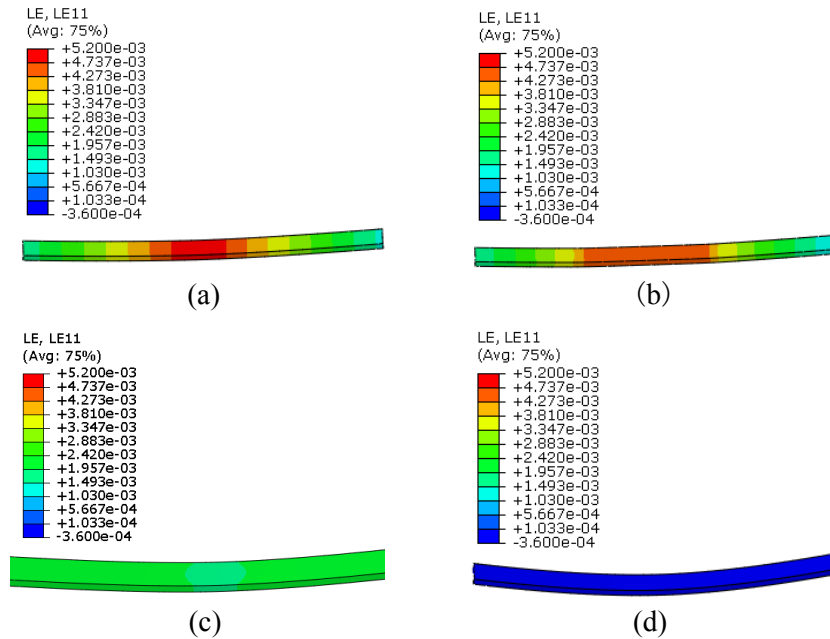


Figure 11: The X-direction strain of the second CFRP sheet at a distance of 150 mm from mid-span: (a) intact, (b) length of debonding 100 mm, (c) length of debonding 500 mm, (d) completely debonded

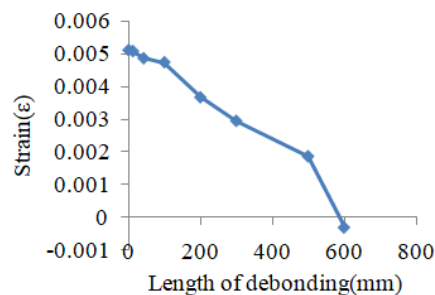


Figure 12: The relationships between LE of the second CFRP at mid-span position and the length of the stripped adhesive layer

Fig. 13 shows the contact pressure on the upper surface of the second CFRP sheet when the adhesive between the second sheet of bamboo scrimber and the second CFRP sheet symmetrically debonds. The maximum contact pressures both are at the mid-span when the total length of the stripped adhesive layer is 100 mm and the adhesive layer is completely stripped. In the former case, the maximum contact pressure of the second CFRP sheet is 2.867 MPa, and in the latter 1.496 MPa, 52.18% of the former. In the former case, the pressure on the upper surface of the second CFRP sheet is still large at a non-intermediate position of the debonding area, and in the latter, the pressure becomes small, maybe because the lower part of the beam is regarded as an independent one after the adhesive layer's completely stripped whose section height is much smaller than the total height of the specimen, and only a small pressure is required to produce a large deformation. Since the contact pressure reduces, the change of X-direction strain of the second CFRP sheet grows smaller, too.

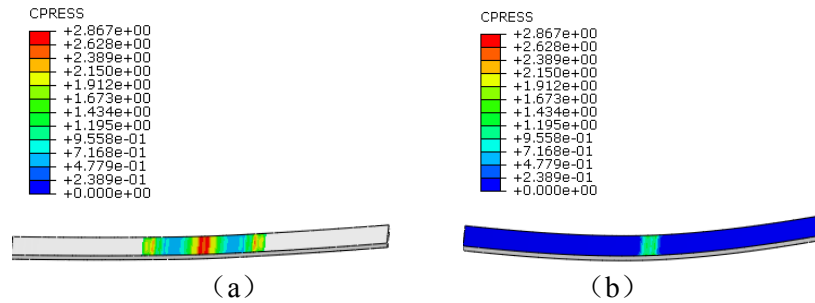


Figure 13: The contact pressure on the second CFRP sheet: (a) the length of debonding 100 mm, (b) completely debonded

The relationships between the deflection of the specimen at mid-span position and the length of the stripped adhesive layer are shown in Fig. 14 where the deflection value goes up at a hiking speed with the length of the stripped adhesive layer, which may be due to the fact that the CBSC beam is no longer an integral once completely debonded. The upper and lower parts can only transmit positive pressure and tangential friction through contact in the debonding area, and normal and tangential loads in the unpeeled area. That is, the load transfer mode of the composite beam gets more complicated.

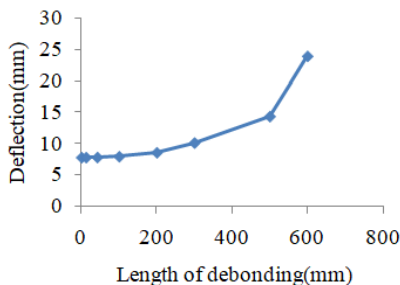


Figure 14: The relationships between the deflection of the specimen at mid-span position and the length of the stripped adhesive layer

5 Conclusions

This study presents a new type of bamboo scrimber beam combining bamboo scrimber sheets and CFRP sheets. Three-point bending test and finite element model were conducted to determine the failure mode, strain-displacement relationship, load-displacement relationship, static flexural modulus, static flexural strength and the effect of adhesive debonding. The research results are as follows:

(1) The failure mode of the CBSC beams was different from that of the bamboo scrimber beams for which the failure started with the bamboo fiber fracture at the mid-span of the lower surface of the beam. But for the CBSC beams, the failure started with the adhesive layer debonding between CFRP sheet and bamboo scrimber sheet.

(2) With the same section, CFRP could help significantly improve the static flexural modulus of the bamboo scrimber beam. The static flexural modulus of the CBSC beams was 2.33-2.94 times the average static flexural modulus of bamboo scrimber beams, related to the location of CFRP layout.

(3) With the same section, the static flexural strength of the CBSC beams was 1.49-1.58 times the average of the bamboo scrimber beams, not as obvious as the static flexural modulus for the adhesive layer debonding.

(4) The deformation process of the bamboo scrimber beams consisted of the linear elastic stage, the stiffness degradation stage and the failure stage, while that of the CBSC beams could be divided into the linear elastic stage and the adhesive layer debonding stage.

(5) When CBSC beams were destroyed, the bamboo scrimber was basically in the linear elastic stage with no stiffness degradation.

(6) The peeling of the adhesive layer had a large impact on the strain and deformation of the CBSC beam. When the adhesive layer completely debonded, the strain distribution of the composite specimen was similar to that of the two separation components, and the deflection was 3.09 times that of the unpeeled one.

Acknowledgment: The project is supported by the Natural Science Foundation of China (Grant No U1737112) and Chinese Postdoctoral Station of Yihua Life Science and Technology Co., Ltd. (No. 201141).

References

1. Sharma, B., Gatóo, A., Bock, M., Ramage, M. (2015). Engineered bamboo for structural applications. *Construction and Building Materials*, 81, 66-73.
2. Yu, W. J. (2019). Current situation and opportunities for the development of bamboo scrimber industry in china. *World Bamboo and Rattan*, 17, 1-4.
3. Fang, C. H., Jiang, Z. H., Sun, Z. J., Liu, H. R., Zhang, X. B. et al. (2018). An overview on bamboo culm flattening. *Construction and Building Materials*, 171, 65-74.
4. Li, H. T., Qiu, Z. Y., Wu, G., Corbi, O., Wang, L. B. et al. (2019). Slenderness ratio effect on eccentric compression performance of parallel strand bamboo lumber columns. *Journal of Structural Engineering ASCE*, 145(8), 04019077.
5. Li, H. T., Chen, G., Zhang, Q., Ashraf, M., Xu, B. et al. (2016). Mechanical properties of laminated bamboo lumber column under radial eccentric compression. *Construction and Building Materials*, 121, 644-652.
6. Huang, Z., Chen, Z., Huang, D., Zhou, A. (2016). The ultimate load-carrying capacity and deformation of laminated bamboo hollow decks: experimental investigation and inelastic analysis. *Construction and Building Materials*, 117, 190-197.
7. Xiao, Y., Chen, G., Feng, L. (2014). Experimental studies on roof trusses made of glulam. *Materials and Structures*, 47(11), 1879-1890.
8. Gottron, J., Harries, K. A., Xu, Q. (2014). Creep behaviour of bamboo. *Construction and Building Materials*, 66, 79-88.
9. Yu, W. J., Yu, Y. L. (2012). Key technology and application of bamboo composites for structural design. *Construction Technology*, 22(3), 55-57.
10. Zheng, J., Shu, B. Q., Xiao, Z. P., Zhong, P. (2017). Advantages and disadvantages of new building material recombinant bamboo's development. *Wood Processing Machinery*, 28(1), 39-42.
11. Luca, V. D., Marano, C. (2012). Prestressed glulam timbers reinforced with steel bars. *Construction and Building Materials*, 30, 206-217.
12. Zhong, Y., Wu, G., Ren, H., Jiang, Z. (2017). Bending properties evaluation of newly designed reinforced bamboo scrimber composite beams. *Construction and Building Materials*, 143, 61-70.
13. Nadir, Y., Nagarajan, P., Ameen, M., Muhammed, A. M. (2016). Flexural stiffness and strength enhancement of horizontally glued laminated wood beams with GFRP and CFRP composite sheets. *Construction and Building Materials*, 112, 547-555.
14. Wei, Y., Wang, X., Li, G. (2014). Mechanical properties test of bamboo scrimber flexural specimens reinforced with bars. *Acta Materiae Compositae Sinica*, 31(4), 1030-1036.
15. Wei, Y., Zhou, M. Q., Chen, D. J. (2015). Flexural behaviour of glulam bamboo beams reinforced with near-surface mounted steel bars. *Materials Research Innovations*, 19(S1), S1-98-S1-103.
16. Wei, Y., Li, G. F., Jiang, S. X., Zhang, Q. S., Lv, Q. F. (2011). Preliminary research on mechanical properties of FRP-reinforced bamboo beams. *Advanced Materials Research*, 243-249, 1237-1241.
17. Zhou, A. P., Liu, R., Shen, Y. R. (2017). Experiment study on ultimate load-bearing capacity of carbon fiber reinforced polymer reinforced parallel bamboo beam. *Journal of Forestry Engineering*, 2(3), 137-142.
18. Zhou, A., Huang, D., Li, H., Su, Y. (2012). Hybrid approach to determine the mechanical parameters of fibers and matrixes of bamboo. *Construction & Building Materials*, 35, 191-196.

19. Huang, D., Bian, Y., Zhou, A., Sheng, B. (2015). Experimental study on stress-strain relationships and failure mechanisms of parallel strand bamboo made from phyllostachys. *Construction and Building Materials*, 77, 130-138.
20. Huang, Z., Chen, Z., Huang, D., Zhou, A. (2016). The ultimate load-carrying capacity and deformation of laminated bamboo hollow decks: experimental investigation and inelastic analysis. *Construction and Building Materials*, 117, 190-197.
21. Wei, Y., Ji, X., Duan, M., Li, G. (2017). Flexural performance of bamboo scrimber beams strengthened with fiber-reinforced polymer. *Construction and Building Materials*, 142, 66-82.
22. Zhang, H. Z., Li, H. T., Corbi, I., Corbi, O., Wu, G. et al. (2018). AFRP influence on parallel bamboo strand lumber beams. *Sensors*, 18, 28-54.
23. Li, H. T., Wu, G., Zhang, Q. S., Deeks, A. J., Su, J. W. (2018). Ultimate bending capacity evaluation of laminated bamboo lumber beams. *Construction and Building Materials*, 160, 365-375.
24. GB/T 50329-2012. Wood structure test. Standards Press of China. 2012.
25. Glišović, I., Stevanović, B., Petrović, M. (2015). Bending behaviour of glulam beams reinforced with carbon FRP plates. *Journal of Civil Engineering and Management*, 21(7), 923-932.